PHYSICAL REVIEW A **77**, 031604(R) (2008)

Measurement of the ac Stark shift with a guided matter-wave interferometer

B. Deissler, K. J. Hughes, J. H. T. Burke, and C. A. Sackett*
Department of Physics, University of Virginia, Charlottesville, Virginia 22904, USA

(Received 26 September 2007; published 14 March 2008)

The dynamic polarizability of ^{87}Rb atoms was measured using a guided-wave Bose-Einstein condensate interferometer. Taking advantage of the large arm separations obtainable in our device, a well-calibrated laser beam is applied to one atomic packet and not the other, inducing a differential phase shift. The technique requires relatively low laser intensity and works for arbitrary optical frequencies. For off-resonant light, the ac polarizability is obtained with a statistical accuracy of 3% and a calibration uncertainty of 6%. On resonance, the dispersion-shaped behavior of the Stark shift is observed, but with a broadened linewidth that is attributed to collective light scattering effects. The resulting nonlinearity may prove useful for the production and control of squeezed quantum states.

DOI: 10.1103/PhysRevA.77.031604 PACS number(s): 03.75.Be, 32.60.+i, 37.25.+k

Atom interferometers are useful for a variety of applications, from the precise measurement of inertial effects to probes of chemical interactions [1,2]. While interference with matter waves in free space has yielded impressive results [3,4], a considerable amount of space is needed for the atoms to fall under the influence of gravity or for an atomic beam to propagate. Using atoms confined in a guiding potential can solve this problem and permits more flexible geometries such as circular rings [5,6]. Guided-wave interferometers have been demonstrated in "proof-of-principle" experiments [7–13], and we here apply one to a practical measurement. We use our interferometer to measure the dynamic polarizability of ^{87}Rb with an estimated accuracy of 7%, a significant improvement over previous interferometric methods [8,14,15]. The accuracy is similar to that of the best noninterferometric technique [16], but in comparison our method requires a factor of 10^2 less laser power and can be used at any optical frequency, including on resonance. Indeed, measurement on resonance reveals the familiar dispersion-shaped dependence, but with a broadened linewidth that we attribute to collective scattering effects [17,18].

In an oscillating electric field E, the energy levels of an atom shift due to the ac Stark effect by an amount $U=-\frac{1}{2}\alpha\langle E^2\rangle$. This effect is relevant to precision measurements, where the magnitude of such shifts must be well known [19,20], and measurements of the polarizability α are important for verifying *ab initio* calculations of dipole matrix elements [21].

Combining the energy shift with the expression for the intensity of a beam of light, $I=c\epsilon_0\langle E^2\rangle$ gives

$$U=-\frac{1}{2c\epsilon_0}\alpha I. \tag{1}$$

Our experiment uses ^{87}Rb, and we operate near the principal transitions from the $5S_{1/2}$, $F=2$ ground state to the $5P_{1/2}$ state at 795 nm, and to the $5P_{3/2}$ state at 780 nm. Second-order perturbation theory gives the polarizability of a ground state $|i\rangle$ as [22]

$$\alpha_i(\omega_\ell)=\frac{2}{\hbar}\sum_{f\neq i}\frac{\omega_f}{\omega_f^2-\omega_\ell^2}|\mu_{if}|^2, \tag{2}$$

where ω_ℓ is the frequency of the applied laser beam, ω_f is the transition frequency to an excited state $|f\rangle$, and μ_{if} is the transition dipole matrix element $\langle i|e\mathbf{r}|f\rangle$. The matrix element is related to the decay rate Γ_{fi} of the excited state by

$$\Gamma_{fi}=\frac{\omega_f^3}{3\pi\epsilon_0\hbar c^3}|\mu_{if}|^2. \tag{3}$$

We use this expression to normalize the dipole moments to the $5P_{3/2}$ $(F=3,m_F=3)\rightarrow 5S_{1/2}$ $(F=2,m_F=2)$ cycling transition rate, where $\Gamma_{33\rightarrow 22}=\Gamma=2\pi\times 6.065$ MHz [23]. Then

$$\alpha_i(\omega_\ell)=4\pi\epsilon_0\frac{3\Gamma c^3}{2\omega_{33}^3}\sum_{f\neq i}\frac{\omega_f}{\omega_f^2-\omega_\ell^2}\left|\frac{\mu_{if}}{\mu_{33}}\right|^2. \tag{4}$$

The ratios of dipole moments are given by standard angular momentum algebra.

Our apparatus has been described in detail before [12,24]. Briefly, we have a Bose-Einstein condensate of 3×10^4 ^{87}Rb atoms in a harmonic waveguide generated by a time-orbiting potential (TOP) with transverse confinement frequencies of 3.3 and 6 Hz and axial confinement at 1.1 Hz. An off-resonant standing-wave laser beam is used to split the condensate into two packets which move in opposite directions along the guide axis with velocity $v_0=11.7$ mm/s [25]. The trajectories are subsequently controlled using reflection pulses, as shown in Fig. 1(a). A symmetric trajectory is used so that the two packets traverse nearly the same path and experience the same phase shifts from the guide potential itself [26,27]. If the packets do acquire a differential phase ϕ, then the the final recombination pulse will bring a fraction of atoms

*sackett@virginia.edu

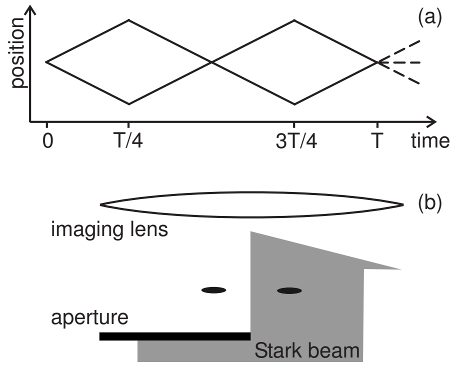

FIG. 1. (a) Trajectory of the atoms in the interferometer. The condensate is split at time $t=0$, reflected at times $T/4$ and $3T/4$, and recombined at time T, all with an off-resonant standing wave laser beam. The atoms are returned to rest by the recombination pulse with a probability that depends on the packets' differential phase. (b) Schematic of the experimental setup. The waveguide axis is in the horizontal direction. The Stark beam is apertured such that it only interacts with one packet of atoms at the maximum separation in the interferometer. This beam is imaged with the same camera used to observe the atoms.

$$\frac{N_0}{N} = \frac{1}{2}(1 + \cos \phi) \tag{5}$$

to rest, while the remainder continue moving at speed v_0. The packets are allowed to separate for a short time and are then probed via absorption imaging.

In the experiments discussed here, the interferometer time is always $T=40$ ms, for which we have about 85% visibility [27]. The maximum center-to-center separation of the two packets is 240 μm, which is significantly larger than the cloud half-width of 55 μm and permits independent access to the two packets. This allows us to apply a laser (the Stark beam) to one atom packet but not the other, as in Fig. 1(b).

The Stark beam is linearly polarized perpendicular to the trap bias field and along the axis of the guide. An acousto-optic modulator (AOM) is used to pulse on the Stark beam for a short time before and after the first reflect pulse, and a mechanical shutter blocks any leakage light from the AOM. The power in the Stark beam is measured during the applied pulse with a photodiode and the intensity corrected accordingly to account for variations over time, which are generally less than 10%. After completing the interferometer sequence and recombining the two clouds, the ratio N_0/N is measured for different intensities and durations of the beam.

We used two different laser frequencies. For the first measurement, seen in Fig. 2(a), the laser was tuned 6.57 GHz red of resonance. In two variations, a 475 μs pulse was applied and the Stark beam intensity I varied from 1 to 15 mW/cm^2, or a beam with intensity 10.5 mW/cm^2 was applied for times t ranging from 0 to 675 μs. We fit the data to a function $f(It)=1/2+\exp(-\beta It)\cos[2\pi(It-x_0)/P]$, where P is the period, x_0 is an overall phase offset, and β is a decay constant reflecting the fact that intensity gradients in the beam induce spatial variations in the phase which eventually wash out the interference. Here the unapertured beam

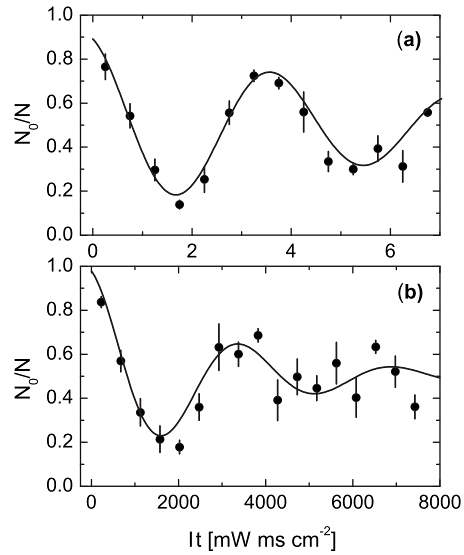

FIG. 2. Measurement of the phase shift from a laser beam at (a) 780.232 nm and (b) 808.37 nm. In both graphs, the solid line indicates a fit to the data. Since there is an increasing phase gradient across the atomic cloud with increasing phase, the visibility decays at higher intensities and longer times. To construct the graphs, we binned together groups of data with a similar product of measured intensity and pulse time. The bin size is 0.5 mW ms cm^{-2} in (a), 450 mW ms cm^{-2} in (b), and the error bars indicate the standard deviation of the mean within the bin.

waist was 1 mm. We extract the polarizabilities from the fit using $|\alpha|=4\pi\epsilon_0 c\hbar/P$. For this data we obtain $|\alpha|=4\pi\epsilon_0\times(8.37\pm0.24)\times10^{-25}$ m^3, where the error is the statistical error from the fit. A theoretical value is obtained by considering transitions from the ground state to the $5P_{3/2}$, $F=2,3$ excited states. The contributions from the Zeeman effect induced by the 20 G trap bias field and from the $5P_{1/2}$ states are negligible. This calculation indicates $|\alpha|=4\pi\epsilon_0\times8.67\times10^{-25}$ m^3, a deviation of +3.5% relative to the experiment.

For the second measurement a free running laser diode at 808.37 nm was used, with applied pulses having intensity ranging from 0 to 6.6 W/cm^2 and duration from 0 to 1.4 ms. The results are seen in Fig. 2(b). For this data, the fit gives $|\alpha|=4\pi\epsilon_0\times(9.48\pm0.25)\times10^{-28}$ m^3. To obtain the higher intensity, the Stark beam was focused to a waist of 0.2 mm, leading to larger gradients across the cloud and thus faster decay of the visibility. A theoretical value was calculated using contributions from transitions to the $6P$ as well as all the $5P$ states. Contributions from the hyperfine structure of the excited states and from higher P states are negligible. This yields an expected value of $|\alpha|$ $=(4\pi\epsilon_0)\times9.14\times10^{-28}$ m^3, differing from the experiment by −3.7%. In both cases, we attribute the deviation between experiment and theory to inaccuracy of the intensity calibration.

As in most measurements of polarizability, the calibration of the applied field is the primary source of uncertainty. In our technique, however, the atoms are well-localized within the Stark beam and a single camera is used to observe both the beam and the atoms. This allows a relatively precise determination of the actual intensity applied. We calibrate the camera by comparing the sum of the pixel values in an image of the beam to the total power as measured by an Ophir PD200 optical power meter. Alternatively, the picture of the unapertured beam can be fit to a two-dimensional Gaussian distribution, and the intensity at the atoms estimated as the value of the Gaussian function. This method averages over high-frequency spatial noise in the beam, some of which is introduced by the imaging optics and thus is not present on the atoms. The intensities obtained with the two methods agree with a standard deviation of 4%, and we use their average for the calibration.

Another source of error is the calibration of the power meter, which has a specified accuracy of 5%. This is consistent with the difference observed when comparing the PD200 to a Coherent Lasermate meter. Altogether, we estimate the total uncertainty for the measurement to be 7%, which can be compared to the 8% error cited by Kadar-Kallen *et al.* [16]. Turning our result around, the fact that the dipole moment for the ^{87}Rb transition is known accurately means that our technique could instead be used as precise measurement of the Stark beam intensity at the atoms, with an uncertainty of about 3%.

We also used the interferometer to measure the ac Stark shift directly at the $5P_{3/2}$, $F=3$ resonance. The dispersion shape of the energy shift through resonance is well known, and can be measured using microwave spectroscopy of the ground state hyperfine transition [28]. However, the atom interferometric technique can be applied also to atoms that lack ground state hyperfine structure. A measurement for a Bose-Einstein condensate is of particular interest due to the possibility for collective line broadening effects [17,18].

In the resonant measurement, we applied the Stark beam with a fixed duration and intensity. To measure the phase shift ϕ, we varied the phase θ of the standing wave during the recombination pulse. The fraction of atoms brought to rest is then $\cos^2(\phi/2-2\theta)$ [12]. We take an interference curve by stepping through θ and obtain ϕ as the offset of the curve. We performed this procedure for various detunings of the Stark beam, with results shown in Fig. 3(a). The error bars are from the fits of the interference curves. The overall offset of -0.3 rad is consistent with the residual phase induced by the guide itself with no Stark beam.

Near resonance, photon scattering cannot be neglected. If an atom absorbs a photon, it leaves the condensate fraction and is lost from the magnetic trap. To avoid losing all the atoms, a relatively low intensity beam ($I\approx 40\ \mu\text{W/cm}^2$) is used that is applied for a short duration (4 μs). The small number of photons makes direct measurement of the intensity difficult. Instead, we measured the atom loss when the experiment is performed without applying the recombination pulse. In this case, we observe just two packets, one of which has been exposed to the Stark beam. From the ratio of the numbers of atoms we can accurately determine the loss. The results are shown in Fig. 3(b), along with a comparison to a calculation for a two-level system [29]. We adjusted the Rabi frequency in the calculation to match the experiment. To obtain good agreement, however, we find that a broadened linewidth of $\Gamma'=2\pi\times(10.0\pm0.9)$ MHz is required, 1.6 times larger than expected. The solid curve in Fig. 3(a) shows the phase shift calculated with these parameters and exhibits the same broadening.

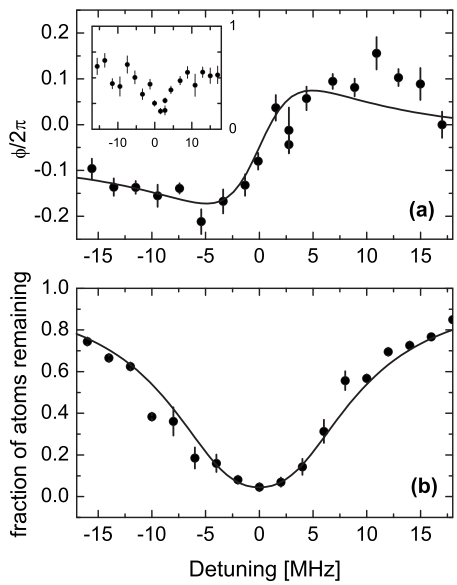

FIG. 3. (a) Measurement of the phase shift from a laser beam near the atomic resonance. The inset shows the visibility of the measured interferometer curve for various detunings of the Stark beam. (b) Loss of atoms due to the beam applied to one packet of atoms. Data in (b) are fit to a functional form $N(t)/N=\exp[-(\Omega^2\Gamma' t)/(\Gamma'^2+4\Delta^2)]$ to determine the Rabi frequency Ω and broadened linewidth Γ'. Here Δ is the detuning and $t=4\ \mu$s is the duration of the laser pulse. The fit, shown as the solid curve, gives $\Omega=2\pi\times1.1$ MHz and $\Gamma'=2\pi\times10.0$ MHz. These values are used in a two-level model to calculate the solid curve in (a).

We confirmed the existence of this broadening by measuring the loss of atoms from a plain condensate after application of a laser beam with different detunings, both in and out of the guide fields. In all cases, the beam intensity was low enough that conventional power broadening was negligible. We do observe a strong intensity dependence, as well as dependence on the atomic density. For noncondensed clouds with low optical density, the unbroadened linewidth is recovered. These effects are being investigated further, and will be described in a future publication.

The broadening might be caused by superradiant scattering [30]. This has been predicted previously for condensates [17,18] and observed for off-resonant light [31]. The predicted linewidth is [17,30]

$$\Gamma' = \frac{3}{2}N\left(\frac{\lambda}{2\pi L}\right)^2\Gamma \tag{6}$$

for a condensate of size L. If we use $L=(L_xL_yL_z)^{1/3}\approx 22\ \mu$m for our Thomas-Fermi widths L_i, we obtain $\Gamma'=1.5\Gamma$, in reasonable agreement with the observations. The effect is observed only for optically thick clouds, typically with resonant optical densities of 2 to 3. It is therefore also possible that multiple photon scattering plays a role.

The presence of collective line broadening has important implications. It means that the phase shift imposed by a near-resonant Stark beam depends on N, which thus provides a source of controllable nonlinearity for the quantum state of the atoms. For instance, condensate interferometers are expected to be limited by atomic interactions [32]. The number of atoms in a packet has unavoidable quantum fluctuations, and thus the interaction energy is uncertain. This in turn imparts an uncertain phase shift that limits the coherence time of the interferometer [13]. However, if a near-resonant Stark beam can provide a number-dependent phase shift, this could be used to correct for the unknown interaction phase and thus recover the coherence time. More generally, any source of nonlinearity can produce squeezed quantum states, which are useful for applications in quantum information [33].

In conclusion, we have used a guided-wave atom interferometer to make high-quality measurements of the ac Stark shift. The method is unique in providing good accuracy, high sensitivity, and operation at arbitrary frequency. The polarizability measured at large detunings was found to agree with theoretical calculations within the experimental accuracy. Measurements at the atomic resonance, however, exhibited a broadened linewidth that we attribute to superradiant scattering, and which may permit nonlinear control of the condensate phase. We plan to extend our measurements to the dc polarizability by inserting one of the packets in between a pair of well-calibrated electric field plates. Through experiments such as these, guided-wave interferometers are beginning to make important contributions to metrology.

We thank T. F. Gallagher for the loan of equipment used in the experiments and R. R. Jones for helpful comments on the manuscript. This work was sponsored by the National Science Foundation (Contract No. PHY-0653349).

[1] *Atom Interferometry*, edited by P. R. Berman (Academic, San Diego, 1996).
[2] K. Bongs and K. Sengstock, Rep. Prog. Phys. **67**, 907 (2004).
[3] T. L. Gustavson, P. Bouyer, and M. A. Kasevich, Phys. Rev. Lett. **78**, 2046 (1997).
[4] C. R. Ekstrom, J. Schmiedmayer, M. S. Chapman, T. D. Hammond, and D. E. Pritchard, Phys. Rev. A **51**, 3883 (1995).
[5] S. Gupta, K. W. Murch, K. L. Moore, T. P. Purdy, and D. M. Stamper-Kurn, Phys. Rev. Lett. **95**, 143201 (2005).
[6] A. S. Arnold, C. S. Garvie, and E. Riis, Phys. Rev. A **73**, 041606(R) (2006).
[7] H. Kreutzmann *et al.*, Phys. Rev. Lett. **92**, 163201 (2004).
[8] Y. Shin *et al.*, Phys. Rev. Lett. **92**, 050405 (2004).
[9] T. Schumm *et al.*, Nat. Phys. **1**, 57 (2005).
[10] S. Wu, E. J. Su, and M. Prentiss, Eur. Phys. J. D **35**, 111 (2005).
[11] Y.-J. Wang *et al.*, Phys. Rev. Lett. **94**, 090405 (2005).
[12] O. Garcia, B. Deissler, K. J. Hughes, J. M. Reeves, and C. A. Sackett, Phys. Rev. A **74**, 031601(R) (2006).
[13] G.-B. Jo *et al.*, Phys. Rev. Lett. **98**, 030407 (2007).
[14] U. Sterr, K. Sengstock, J. H. Müller, D. Bettermann, and W. Ertmer, Appl. Phys. B: Photophys. Laser Chem. **B54**, 341 (1992).
[15] A. Morinaga, T. Tako, and N. Ito, Phys. Rev. A **48**, 1364 (1993).
[16] M. A. Kadar-Kallen and K. D. Bonin, Phys. Rev. Lett. **68**, 2015 (1992).
[17] J. Javanainen, Phys. Rev. Lett. **72**, 2375 (1994).
[18] L. You, M. Lewenstein, R. J. Glauber, and J. Cooper, Phys. Rev. A **53**, 329 (1996).
[19] C. E. Wieman, M. C. Noecker, B. P. Masterson, and J. Cooper, Phys. Rev. Lett. **58**, 1738 (1987).
[20] P. R. Hemmer, M. S. Shahriar, V. D. Natoli, and S. Ezekiel, J. Opt. Soc. Am. B **6**, 1519 (1989).
[21] M. S. Safronova and C. W. Clark, Phys. Rev. A **69**, 040501(R) (2004).
[22] C. Cohen-Tannoudji, B. Diu, and F. Laloë, *Quantum Mechanics*, 2nd ed. (Hermann, Paris, 1977).
[23] U. Volz and H. Schmoranzer, Phys. Scr. **T65**, 48 (1996).
[24] J. M. Reeves *et al.*, Phys. Rev. A **72**, 051605(R) (2005).
[25] K. J. Hughes, B. Deissler, J. H. T. Burke, and C. A. Sackett, Phys. Rev. A **76**, 035601 (2007).
[26] J. A. Stickney, D. Z. Anderson, and A. A. Zozulya, Phys. Rev. A **75**, 063603 (2007).
[27] J. H. T. Burke, B. Deissler, K. J. Hughes, and C. A. Sackett, e-print arXiv:710.1081.
[28] A. Kastler, J. Opt. Soc. Am. **53**, 902 (1963).
[29] C. Cohen-Tannoudji, J. Dupont-Roc, and G. Grynberg, *Atom-Photon Interactions: Basic Processes and Applications* (Wiley, New York, 1992).
[30] M. Gross and S. Haroche, Phys. Rep. **93**, 301 (1982).
[31] S. Inouye *et al.*, Science **285**, 571 (1999).
[32] J. Javanainen and M. Wilkens, Phys. Rev. Lett. **78**, 4675 (1997).
[33] R. Loudon, *The Quantum Theory of Light* (Oxford University Press, Oxford, 2000), 3rd ed.